

# Room-Temperature Ferromagnetism in Perylene Diimide Organic Semiconductor

Qinglin Jiang, Jiang Zhang,\* Zhongquan Mao, Yao Yao,\* Duokai Zhao, Yanhua Jia, Dehua Hu,\* and Yuguang Ma\*

The development of pure organic magnets with high Curie temperatures remains a challenging task in material science. Introducing high-density free radicals to strongly interacting organic molecules may be an effective method to this end. In this study, a solvothermal approach with excess hydrazine hydrate is used to concurrently reduce and dissolve rigid-backbone perylene diimide (PDI) crystallites into the soluble dianion species with a remarkably high reduction potential. The as-prepared PDI powders comprising radical anion aggregates are fabricated by a subsequent self-assembly and spontaneous oxidation process. The results of magnetic measurements show that the PDI powders exhibit room-temperature ferromagnetism and a Curie temperature higher than 400 K, with a vast saturation magnetization that reaches  $\approx 1.2 \text{ emu g}^{-1}$ . Elemental analysis along with the diamagnetic signal of the ablated residue are used to rule out the possibility that the magnetism is due to metal contamination. The findings suggest that the long-range ferromagnetic ordering can survive at room-temperature in organic semiconductors, and offers a new optional way to create room-temperature magnetic semiconductors.

Therefore, intrinsic ferromagnetic semiconductors that work at room temperature are rare.<sup>[8]</sup>

Organic ferromagnets with the flexibility, low-temperature synthesis, low density, and biocompatibility take advantage of replacing conventional magnets.<sup>[11–13]</sup> Extensive effort has been devoted to discovering ferromagnetism in purely organic semiconductors based on the radicals.<sup>[14,15]</sup> In 1963, McConnell<sup>[16]</sup> first pointed out that aromatic and olefinic free radicals may pancake on top of one another in the crystalline lattice and give rise to a ferromagnetic exchange interaction between  $\pi$ -electron spins by favoring a parallel spin angular momentum on the neighboring molecules. Until 1991, the first example of an organic ferromagnet without metal elements was found in *p*-nitrophenyl nitronyl nitroxide crystal,<sup>[17]</sup> in which the exchange of free radical electrons between neighboring molecules

causes the spins to become parallel. The inherent magnetic moment with parallel spin has a long range order in the lattice, and exhibits ferromagnetic properties with a saturated magnetization of  $10.1 \text{ emu g}^{-1}$ , while its  $T_c$  is only 0.6 K. Subsequently, Rawson et al.<sup>[18]</sup> regulated the molecular aggregation through the substitution of cyanide and fluorine atoms, increasing the  $T_c$  to 36 K in the  $\beta$  phase crystal of the dithiadiazolyl radical. In almost all cases, such molecular interactions have proved to be weak, thus making the ferromagnetic phase observable only at very low temperatures.<sup>[19–21]</sup> Charge transfer organic crystal, such as tetrathiafulvalene (TTF)-C<sub>60</sub><sup>[22]</sup> and coronene-tetracyanoquinodimethane (TCNQ)<sup>[23]</sup> exhibited very weak ferromagnetism at room-temperature. Recently, Baek et al.<sup>[24]</sup> reported an insulating polymeric organic magnet in the self-polymerized TCNQ framework. Owing to the limited degree of order of the cross-linked conjugate aggregates, this material displayed weak ferromagnetism (the saturation magnetization was only of the order of  $10^{-3} \text{ emu g}^{-1}$ ) at room-temperature. Nevertheless, room-temperature ferromagnetism, along with semiconducting properties in the organic materials composed merely of carbon, hydrogen, oxygen, and nitrogen, have hitherto not been found.


As a widely investigated n-type semiconductor, perylene diimide (PDI) serves as a promising candidate in various optoelectronic devices, including thin-film transistors, photovoltaics, thermoelectric, and light-emitting diodes.<sup>[25–30]</sup> The PDI molecule comprises a perylene backbone with two imide

## 1. Introduction

In the early scenario in quantum mechanics, ferromagnetism was thought to arise from electrons with principal quantum numbers greater than two.<sup>[1]</sup> Naturally, magnetic semiconductors, such as undoped magnetic semiconductors<sup>[2,3]</sup> and diluted magnetic semiconductors,<sup>[4,5]</sup> are mostly based on metal elements. Diluted magnetic semiconductors allow the coupling and dependently controlling of electron charge and spin,<sup>[6,7]</sup> while they yet confront several fundamental challenges, including low Curie temperature ( $T_c$ ), magnetic impurity, distribution, and solubility limit of the magnetic metal ions.<sup>[8–10]</sup>

Q. Jiang, J. Zhang, Y. Yao, D. Zhao, Y. Jia, D. Hu, Y. Ma  
State Key Laboratory of Luminescent Materials and Devices  
South China University of Technology  
Guangzhou 510640, China  
E-mail: jonney@scut.edu.cn; yaoyao2016@scut.edu.cn;  
msdhhu@scut.edu.cn; ygma@scut.edu.cn

J. Zhang, Z. Mao, Y. Yao  
Department of Physics  
South China University of Technology  
Guangzhou 510640, China

 The ORCID identification number(s) for the author(s) of this article can be found under <https://doi.org/10.1002/adma.202108103>.

DOI: 10.1002/adma.202108103

end-groups. Owing to the strong intermolecular  $\pi$ - $\pi$  interaction and hydrogen bonding, the pristine PDI tends to crystallize and suffer poor solubility in commonly used organic solvents, impeding the manufacturing of solution-processable organic thin-film devices.<sup>[31]</sup> With four electron-withdrawing carbonyl groups, the PDI molecule can be reduced to metastable radical anions or dianions through electrochemical or chemical reduction.<sup>[32,33]</sup> Therefore, PDI can form tightly packed aggregates of radical anion, and may acquire ferromagnetic properties.

Here, we reduced and dissolved the PDI crystallites by using the solvothermal approach to fabricate self-assembling PDI nanorods. The unprecedented room-temperature ferromagnetism in organic semiconductor was confirmed through magnetic measurements. The possible contributions of the very few metal impurities present were carefully excluded. Owing to the negligible spin-orbital couplings and, thus, the long spin lifetime in organic materials, we argue that the results will shed a light on the realization and application of room-temperature magnetic semiconductors.

## 2. Results and Discussion

We conducted a reduction and dissolution treatment of the sublimated PDI crystallites at a  $\pi$ - $\pi$  stacking distance of 3.34 Å (Figure S1a, Supporting Information) by using the solvothermal method with excess hydrazine hydrate (Figure 1a). A purple suspension was obtained after cooling, and was subsequently used to prepare the PDI powders through heating in the glove box ( $H_2O$  &  $O_2 < 1$  ppm) (see the Experimental Section). Benefitting from the intrinsic semiconducting features, the UV-vis absorption spectra were employed to measure the valence states. The main absorption peak at 554 nm indicated that the PDI dianion species dominated the suspension (Figure 1b).<sup>[26,33]</sup> In order to get the electronic structure of PDI dianion, the spin density distributions were calculated by Gaussian 16 and illustrated as surface maps (Figure S1b, Supporting Information). Two radicals with opposite spin located on the C-O bond were graphically shown. The peaks of the as-prepared film appeared at 773, 810, and 965 nm, and helped to identify the production of the PDI radical anions.<sup>[33]</sup> The

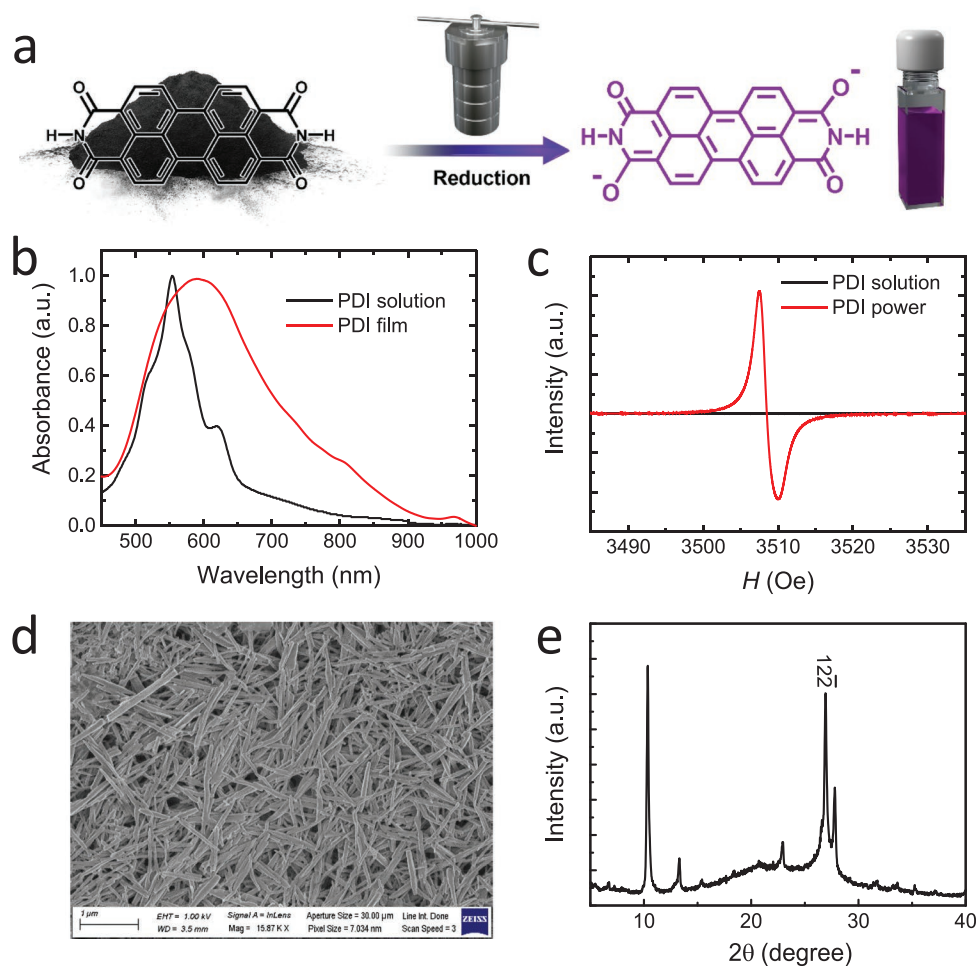


**Figure 1.** Structure characterization. a) Fabrication of PDI solution. The PDI was reduced by hydrazine hydrate through hydrothermal method in a sealed autoclave. b) UV-vis absorption spectra of the purple solution in hydrazine hydrate and the as-prepared PDI film. c) EPR spectra of the PDI solution and the as-prepared PDI powders. d) Scanning electron microscopy image of PDI nanorods with widths of 50–60 nm. e) XRD patterns of the as-prepared PDI powders. The (12 $\bar{2}$ ) diffraction peak was identified as the  $\pi$ - $\pi$  stacking.

electron paramagnetic resonance (EPR) spectra were used to probe the formation of radical anions in the PDI powders. A strong resonance signal around  $g = 2.003$  was observed, and had originated from unpaired electrons, clearly indicating the drastic increase in radical anions after oxidation (Figure 1c). It should be noted that free radicals usually were produced by doping process, which results in the addition of dopants that affect the packing density and degree of ordering.<sup>[21]</sup> In this work, oxygen is used as a dopant to preserve its aggregation structure. The scanning electronic microscopy (SEM) photograph of the PDI powders displayed compactly stacked self-assembly nanorods 50–60 nm wide (Figure 1d). The X-ray diffraction (XRD) pattern of as-prepared PDI powders is shown Figure 1e. The peak around  $26.9^\circ$  can be indexed as  $(12\bar{2})$ , which is corresponding to  $\pi$ - $\pi$  stacking, and the calculated distance was 3.30 Å (Figure 1e). It was essential that the  $\pi$ - $\pi$  stacking remained close after the reduction process, given that the PDI species were ionized.

It is worth mentioning that, in contrast to previous strategies in which the radicals are obtained by a reduction process,<sup>[32,33]</sup> our self-doping approach for radical anions was conducted with a spontaneous oxidation process from closed-shell dianions. Consequently, the self-assembling PDI aggregates synthesized by using this approach are unique in two aspects: the close  $\pi$ - $\pi$  stacking distance and the large concentration of radical anions, which may introduce a strong spin exchange interaction between the radicals and enable a ferromagnetic ordering to eventually emerge.

We investigated the magnetic properties of the PDI semi-conductors using a vibrating sample magnetometer (see the Experimental Section). The magnetization–magnetic field ( $M$ - $H$ ) curves recorded at 10 and 300 K showed representative ferromagnetic hysteresis loops (Figure 2a). The magnetization was saturated at 1.5 kOe, and the coercive field reached 160 Oe at 300 K. The extracted saturated magnetization at 300 K was  $\approx 1.2$  emu  $g^{-1}$ , which is distinctly large in organic magnets and far beyond the 36 K of canting ferromagnets,<sup>[18]</sup> as well as recently reported weak ferromagnets in amorphous polymerized TCNQ<sup>[24]</sup> and 1,3,5-triazine-linked porous organic radical frameworks.<sup>[34]</sup> Furthermore, we measured the hysteresis loops within the temperature range of 10–400 K, and the temperature dependence of the coercive field ( $H_c$ ) suggested ferromagnetism above room-temperature (Figure 2b). The temperature dependence of magnetization in zero-field-cooled (ZFC) and field-cooled (FC) conditions under a magnetic field of 100 Oe is displayed in Figure 2c. The bifurcation between the plots of ZFC and FC starts from 400 K, indicating that the value of  $T_c$  of the ferromagnetic PDI powders was above 400 K. In Figure 2d, the saturated magnetization versus  $T_c$  in purely organic magnets<sup>[18,24,34–36]</sup> are plotted, it can be seen that room-temperature PDI ferromagnet preponderate in both sides of  $T_c$  and saturated magnetization, indicating the potential to be comparable with inorganic ferromagnetic materials in the future. Magnetic response of PDI ferromagnetic powders could be shown vividly through attracting effect by a strong permanent magnet (Video S1, Supporting Information).

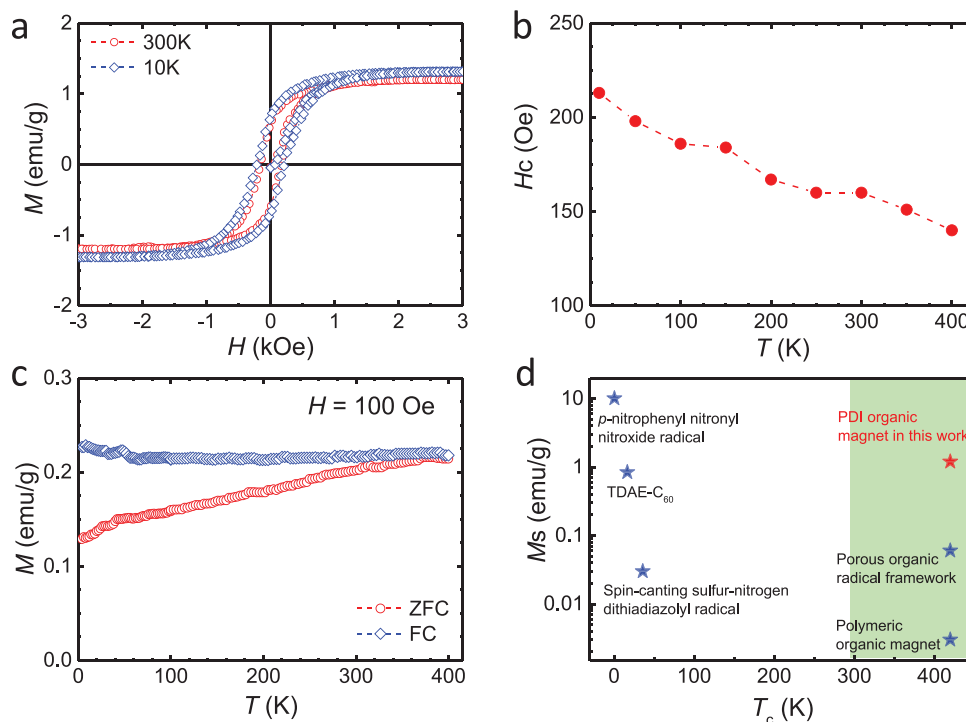


**Figure 2.** Magnetic properties of PDI powders. a) The  $M$ - $H$  hysteresis loops of PDI powders taken at 10 and 300 K. The loops exhibit coercive fields of 160 Oe at 300 K and 213 Oe at 10 K. b) Temperature dependence of the coercive fields, and suggesting ferromagnetism above room-temperature. c) Curves of ZFC and FC magnetization with temperature, measured at an applied magnetic field of 100 Oe. The bifurcation between the curves of ZFC and FC implies that the Curie temperature of the PDI powders was beyond 400 K. d) The saturated magnetization ( $M_s$ ) versus  $T_c$  in purely organic magnets.<sup>[18,24,34–36]</sup>

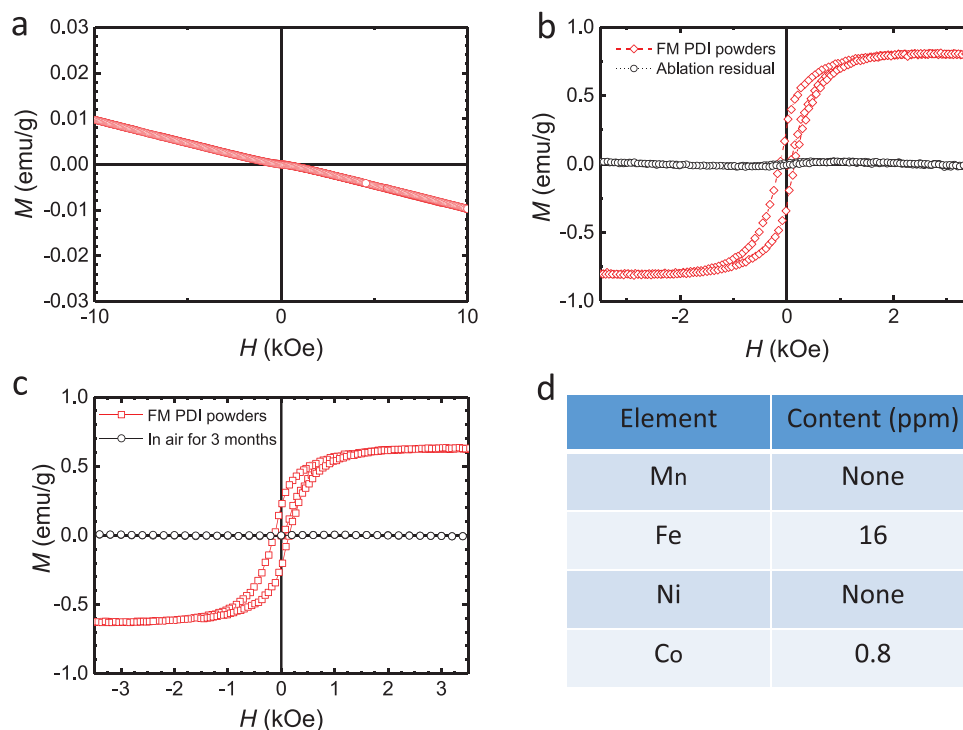


**Figure 3.** Evolution of magnetic properties and metal impurities elemental analysis for ferromagnetic (FM) PDI powders. a) Linear  $M$ - $H$  curves of PDI raw material recorded at 300 K, indicating a diamagnetic behavior. b) The  $M$ - $H$  hysteresis curve of the FM PDI powders with a room-temperature saturation magnetization of  $\approx 0.8 \text{ emu g}^{-1}$  and the  $M$ - $H$  curve of the ablation residual, indicating weak diamagnetism. c) Evolution of magnetic properties for FM PDI powders with time in ambient air. d) Metal impurities elemental analysis by PIXE for ferromagnetic PDI powders. The saturation magnetization contribution of these metal impurities to the sample is no more than  $5 \times 10^{-3} \text{ emu g}^{-1}$ , which is far smaller than the measured value in our experiments.

For a comparison, the linear  $M$ - $H$  curve of the raw PDI material showed diamagnetic features (Figure 3a). This strongly suggests that ferromagnetic signals arose from our reduction and air oxide process. To further rule out the possibility that the ferromagnetism had arisen owing to a very small amount of metal contaminant, we selected a sample with a room-temperature saturation magnetization of  $0.8 \text{ emu g}^{-1}$  for an ablation experiment in the air. Figure 3b shows the  $M$ - $H$  graph of the sample before and after the ablation experiment. It is clear that the ferromagnetism of the sample disappeared after ablation, and the ablated residue showed weak diamagnetism. This eliminates the possibility that the ferromagnetism of the sample was rooted in a ferromagnetic metal or its oxide. We also found that after about 3 months, the ferromagnetism changed to diamagnetism when the sample was continuously exposed to air (Figure 3c). Due to the natural chemical activity of radicals, previously reported organic ferromagnetic crystals are usually unstable, such as TDAE- $C_{60}$ , which would completely lose magnetic properties after exposure to the air by accident for a few seconds.<sup>[19]</sup> Compared with this low  $T_c$  organic ferromagnets, our ferromagnetic powders showed higher stability in air. The amount of magnetic metallic impurities in our sample, as measured by particle-induced X-ray emission (PIXE) spectra, was far from sufficient to induce the ferromagnetic signal (Figure 3d). All these experiment data suggest with greater certainty that the observed ferromagnetism was intrinsically derived from the PDI radical crystals.

To investigate the semiconducting properties of the samples, we measured the temperature dependence of the resistance and the Hall coefficient at 300 K. The devices used for the measurements were made using the geometry of a six-contact Hall bar, and the optical microscopy images of the top view of the Hall devices appear in Figure 4a. The resistivity,  $\rho$ , was extracted from the longitudinal resistance in the ohmic response regime. As shown in Figure 4b, the curve of resistance versus temperature showed typical semiconductor features. At room-temperature, the resistivity was  $\approx 1.6 \text{ } \Omega \text{ cm}$ . In Figure 4c, we fitted the temperature dependent resistance data according to an Arrhenius equation  $R = R_0 e^{-E_a/k_B T}$ , which give the activation energy  $E_a \approx 72.54 \text{ meV}$ . Figure 4d shows that the negative Hall voltage ( $V_H$ ) (i.e., n-type conduction) was linearly proportional to the applied magnetic field, which was determined by:  $V_H = V_H(B) - V_H(0)$ .  $R_H$  is Hall coefficient, extracted from the expression  $R_H = V_H t / (IB)$ , where  $R_H$ ,  $I$ ,  $B$ , and  $t$  are the Hall coefficient, applied current, thickness of the sample, and the applied field, respectively. The Hall mobility,  $\mu_H$ , was calculated from the expression  $\mu_H = R_H / \rho$  at 300K was  $\approx 0.5 \text{ cm}^2 \text{ V}^{-1} \text{ s}^{-1}$ . Combined with the observed ferromagnetism, this PDI radical crystals have enormous potential to achieve the room-temperature magnetic semiconductor ultimately.

We illustrate the process of formation of the metastable radical anions in our sample as follows: The raw material was in the neutral state, and was thoroughly reduced to the dianion state with a high reduction potential through our solvothermal approach. Both states had a closed-shell structure and exhibited

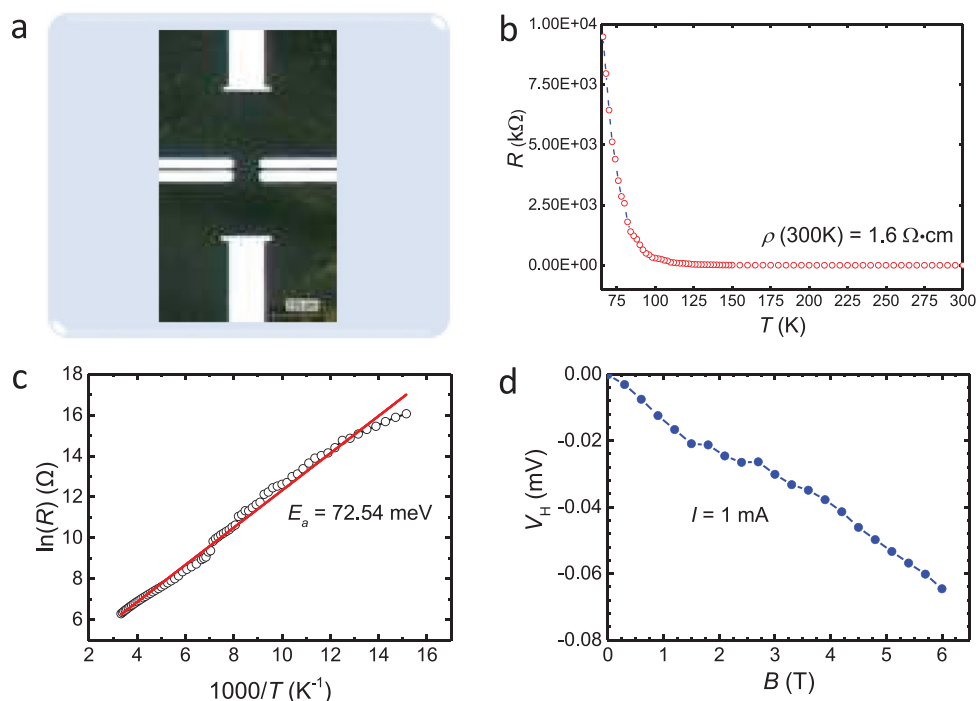


**Figure 4.** Semiconducting properties of PDI ferromagnets. a) Optical microscopy image of the top view of six-contact Hall bar devices. b) Temperature dependence of the resistance of the PDI devices. c) The fitting of temperature dependent resistance data to an Arrhenius equation extracts activation energy  $E_a \approx 72.54$  meV. d) The dependence of  $V_H$  on the magnetic field for the devices, indicating n-type conduction.

diamagnetism. We used the electrochemical method to determine the redox potentials of the dianion, the radical anion, and the neutral state (Figure S2, Supporting Information). In this energy-descending configuration, the sample was spontaneously oxidized in air to produce the neutral state through an intermediate radical anion state with an open-shell structure (Figure S3a, Supporting Information), which afforded unpaired electrons to facilitate the emergence of ferromagnetism. Interestingly, the generation of the neutral state activated a second reaction path to generate the radical anions, namely, one whereby the electron could transfer from the dianion state to the neutral state if the molecules were sufficiently close to one another (Figure S3b, Supporting Information). The radical anions produced by the second reaction initially had a singlet spin configuration because the reactants had a closed-shell structure. With the effect of zero-field splitting,<sup>[37]</sup> the triplet was generated through a spin flip process, and was inhibited from reverting to the neutral and dianion state owing to the spin-forbidden transition. In a short duration, the detailed balance of three components was reached.

Room-temperature ferromagnetism has been rarely observed in semiconductors.<sup>[7]</sup> According to Néel's local molecular field theory,<sup>[38]</sup> when the average radius of the open shell is roughly half the inter-atomic distance, the exchange integral is positive, and gives rise to ferromagnetic exchange interactions. Through our unique synthesis-based approach, the PDI molecules were assembled into nanorods and the  $\pi$ - $\pi$  stacking was kept close, enabling sufficiently strong ferromagnetic spin exchange interactions among the radicals.<sup>[16,37]</sup> Our preliminary calculations show that with the  $\pi$ - $\pi$  distance of 3.32 Å the spin interaction between two PDI radicals is  $\approx 0.02$  cm<sup>-1</sup>, which is compared to

the coercive field observed in our experiment (Figure S4, Supporting Information). In this circumstance, the emergence of spontaneous magnetization can be illustrated using two possible theoretical models based upon localized and itinerant (delocalized) electrons. The first one was proposed by Heisenberg<sup>[1]</sup> and refers to the direct or indirect exchange of local magnetic moments. The second one is from Stoner's picture,<sup>[39,40]</sup> in which the energy band is spontaneously spin-split. In  $\pi$ -conjugated organic crystallites, the electrons are regarded as delocalized to form band-like transport channels but owing to the strong vibronic couplings, the electrons are also easily localized.<sup>[41]</sup> These dual features of localization and delocalization of unpaired electrons in radical anions may cooperatively give rise to the long-range ferromagnetic ordering in PDI semiconductors. Based on our experimental results, ferromagnetism is expected to be found in other free radical molecular crystals with strong  $\pi$ - $\pi$  interaction. In fact, we used a similar approach successfully to produce room-temperature ferromagnetism in naphthalene diimide molecules, which will be published elsewhere.

### 3. Conclusion

Organic semiconductors, especially open-shell polycyclic hydrocarbons with metastable radicals and a close stacking structure, were demonstrated here as a promising candidate for room-temperature ferromagnets. We anticipate that this novel material will be useful for investigating fundamental spin behaviors in organic semiconductors, and can offer the means to explore such applications as pure organic spin devices.

## 4. Experimental Section

**Sample Preparation:** PDI (98%) was purchased from J & K Co., Ltd. Sublimation technology was used to obtain pure PDI (>99%). Hydrazine hydrate (98% in water) was obtained from the Beijing Chemical Plant (Beijing, China). PDI (0.5 mg) and 5 mL of hydrazine hydrate were sealed in an autoclave and heated for 24 h at 140 °C. The autoclave containing the dianion solution was opened in an N<sub>2</sub> glovebox (H<sub>2</sub>O & O<sub>2</sub> < 1 ppm). A high-resistance 10 × 10 mm silicon wafer with a (111) orientation was subsequently cleaned with sonication in water, cleaning agent, acetone, and isopropanol. The films and powders were drop casted from the solutions described above and annealed in the glovebox on a hot plate for 60 min at 80 °C.

**Structure Characterization:** The crystallinity of the samples was characterized using XRD (Rigaku SmartLab) with Cu Ka ( $k = 0.15418$  nm) radiation. The nanostructures were characterized by using a field-emission scanning electron microscope (ZEISS, Oberkochen, Germany) at room-temperature. The UV–vis–NIR characterization was performed on a SHIMADZU UV-3600 spectrophotometer (Kyoto, Japan). EPR spectra were recorded on a Bruker E500 EPR spectrometer (300 K, 9.854 GHz, X-band, Karlsruhe, Germany). The microwave power used was 6.325 mW and the width of the magnetic field sweep ranged from 3267 to 3766 Oe. The modulation frequency was 100 kHz and its amplitude was 5 Oe. Cyclic voltammograms were acquired using a three-electrode system (CHI600E, Shanghai Chenhua). External beam PIXE experiments were carried out at the GIC4117 1.7-MV tandem accelerator at Beijing Normal University.

**Physical Properties Measurement:** Magnetization was measured using Quantum Design PPMS-9 with a vibrating sample magnetometer over the temperature range of 2–400 K. The diamagnetic correction was performed using diamagnetic susceptibility from the sample holder. The resistance and Hall resistivity were measured by a six-contact Hall bar device by Quantum Design PPMS with Electrical Transport Option.

## Supporting Information

Supporting Information is available from the Wiley Online Library or from the author.

## Acknowledgements

Q.J., J.Z., and Z.M. contributed equally to this work. This work was financially supported by the Natural Science Foundation of China (Nos. U20A6002, 91833304, 21973081, 51521002, 21473211, 11574052, and 91833305), National Key R&D Program of China (No. 2020YFA0714604), the Basic and Applied Basic Research Major Program of Guangdong Province (No. 2019B030302007), Research and Development Funds for Science and Technology Program of Guangzhou (No. 202007020004), the Natural Science Foundation of Guangdong Province (No. 2019B121205002), Guangdong Provincial Key Laboratory of Luminescence from Molecular Aggregates (No. 2019B030301003), and Fundamental Research Funds of State Key Laboratory of Luminescent Materials and Devices (No. Skllmd-2021-07). The authors thank for the assistance of theoretical calculation from Jiani Liu, Department of Physics, South China University of Technology.

## Conflict of Interest

The authors declare no conflict of interest.

## Data Availability Statement

The data that support the findings of this study are available from the corresponding author upon reasonable request.

## Keywords

organic semiconductors, perylene diimide, room-temperature ferromagnetism

Received: October 9, 2021  
Revised: December 20, 2021  
Published online:

- [1] W. Heisenberg, *Z. Phys.* **1928**, 49, 619.
- [2] B. T. Matthias, R. M. Bozorth, J. H. Van Vleck, *Phys. Rev. Lett.* **1961**, 7, 160.
- [3] A. Mauger, C. Godart, *Phys. Rep.* **1986**, 141, 51.
- [4] J. K. Furdyna, *J. Appl. Phys.* **1988**, 64, R29.
- [5] H. Ohno, *Science* **1998**, 281, 951.
- [6] K. Sato, L. Bergqvist, J. Kudrnovský, P. H. Dederichs, O. Eriksson, I. Turek, B. Sanyal, G. Bouzerar, H. Katayama-Yoshida, V. A. Dinh, T. Fukushima, H. Kizaki, R. Zeller, *Rev. Mod. Phys.* **2010**, 82, 1633.
- [7] T. Dietl, H. Ohno, *Rev. Mod. Phys.* **2014**, 86, 187.
- [8] K. Ando, *Science* **2006**, 312, 1883.
- [9] N. Samarth, *Nat. Mater.* **2010**, 9, 955.
- [10] S. Chambers, *Nat. Mater.* **2010**, 9, 956.
- [11] J. S. Miller, A. J. Epstein, *MRS Bull.* **2000**, 25, 21.
- [12] J. S. Miller, *Adv. Mater.* **1994**, 6, 322.
- [13] R. M. White, *Science* **1985**, 229, 11.
- [14] J. S. Miller, *Mater. Today* **2014**, 17, 224.
- [15] S. J. Blundell, F. L. Pratt, *J. Phys.: Condens. Matter* **2004**, 16, R771.
- [16] H. M. McConnell, *J. Chem. Phys.* **1963**, 39, 1910.
- [17] M. Tamura, Y. Nakazawa, D. Shiomi, K. Nozawa, Y. Hosokoshi, M. Ishikawa, M. Takahashi, M. Kinoshita, *Chem. Phys. Lett.* **1991**, 186, 401.
- [18] A. J. Banister, N. Bricklebank, I. Lavender, J. M. Rawson, C. I. Gregory, B. K. Tanner, W. Clegg, M. R. J. Elsegood, F. Palacio, *Angew. Chem., Int. Ed.* **1996**, 35, 2533.
- [19] P. M. Allemand, K. C. Khemani, A. Koch, F. Wudl, K. Holczer, S. Donovan, G. Grüner, J. D. Thomopson, *Science* **1991**, 253, 301.
- [20] R. Chiarelli, M. A. Novak, A. Rassat, J. L. Tholence, *Nature* **1993**, 363, 147.
- [21] R. J. Bushby, D. Gooding, M. E. Vale, *Philos. Trans. R. Soc., A* **1999**, 357, 2939.
- [22] B. B. Xu, Z. P. Luo, A. J. Wilson, K. Chen, W. X. Gao, G. L. Yuan, H. D. Chopra, X. Chen, K. A. Willets, Z. Dauter, S. Q. Ren, *Adv. Mater.* **2016**, 28, 5322.
- [23] M. M. Wei, K. P. Song, Y. Y. Yang, Q. K. Huang, Y. F. Tian, X. T. Hao, W. Qin, *Adv. Mater.* **2020**, 32, 2003293.
- [24] J. Mahmood, J. Park, D. Shin, H. J. Choi, J. M. Seo, J. W. Yoo, J. B. Baek, *Chem* **2018**, 4, 2357.
- [25] F. Würthner, *Chem. Commun.* **2004**, 1564.
- [26] Q. L. Jiang, H. D. Sun, D. K. Zhao, F. L. Zhang, D. H. Hu, F. Jiao, L. Q. Qin, V. Linseis, S. Fabiano, X. Crispin, Y. G. Ma, Y. Cao, *Adv. Mater.* **2020**, 32, 2002752.
- [27] H. Usta, A. Facchetti, T. J. Marks, *Acc. Chem. Res.* **2011**, 44, 501.
- [28] L. Zhang, I. Song, J. Ahn, M. Han, M. Linares, M. Surin, H. J. Zhang, J. H. Oh, J. B. Lin, *Nat. Commun.* **2021**, 12, 142.
- [29] M. Li, L. S. Yang, Y. Y. Zhou, Y. H. Liu, J. S. Song, H. Wang, Z. S. Bo, *J. Phys. Chem. C* **2021**, 125, 10841.
- [30] J. Yao, B. B. Qiu, Z. G. Zhang, L. W. Xue, R. Wang, C. F. Zhang, S. S. Chen, Q. J. Zhou, C. K. Sun, C. Yang, M. Xiao, L. Meng, Y. F. Li, *Nat. Commun.* **2020**, 11, 2726.

- [31] K. Balakrishnan, A. Datar, T. Naddo, J. L. Huang, R. Oitker, M. Yen, J. C. Zhao, L. Zang, *J. Am. Chem. Soc.* **2006**, *128*, 7390.
- [32] X. Q. Cao, Y. S. Wu, H. B. Fu, J. N. Yao, *J. Phys. Chem. Lett.* **2011**, *2*, 2163.
- [33] R. O. Marcon, S. Brochsztain, *J. Phys. Chem. A* **2009**, *113*, 1747.
- [34] H. Phan, T. S. Heng, D. G. Wang, X. Li, W. D. Zeng, J. Ding, K. P. Loh, A. T. Shen Wee, J. S. Wu, *Chem* **2019**, *5*, 1223.
- [35] M. Kinoshita, *Philos. Trans. R. Soc., A* **1999**, *357*, 2855.
- [36] K. Tanaka, A. A. Zakhidov, K. Yoshizawa, K. Okahara, T. Yamabe, K. Yakushi, K. Kikuchi, S. Suzuki, I. Ikemoto, Y. Achiba, *Phys. Rev. B* **1993**, *47*, 7554.
- [37] M. Gouterman, W. Moffitt, *J. Chem. Phys.* **1959**, *30*, 1107.
- [38] L. Néel, *Ann. De phys.* **1936**, *5*, 232.
- [39] E. C. Stoner, *Proc. R. Soc. London, Ser. A* **1938**, *165*, 372.
- [40] E. C. Stoner, *Proc. R. Soc. London, Ser. A* **1939**, *169*, 339.
- [41] V. Coropceanu, J. Cornil, D. A. da Silva Filho, Y. Olivier, R. Silbey, J.-L. Brédas, *Chem. Rev.* **2007**, *107*, 926.